ELSEVIER

PII: S0032-3861(96)01064-6

Polymer Vol. 38 No. 11, pp. 2595–2602, 1997

0032-3861/97/$17.00 + 0.00

Photon diffusion and energy transfer processes during chain interdiffusion in films formed from fluorescence labelled high-*T* latex particles

M. Canpolat and Ö. Pekcan*
Department of Physics, Istanbul Technical University, Maslak, 80626, Istanbul, Turkey
(Received 2 October 1995)

Steady state fluorescence (SSF) in conjunction with Monte Carlo simulations was used to study interdiffusion of polymer chains across the particle–particle junction, during film formation from high-T latex particles. The latex films were prepared from pyrene (P) and naphthalene (N) labelled poly (methyl methacrylate) particles, and annealed in elevated time intervals above the glass transition temperature (T_g) at 180°C. Scanning electron microscopy (SEM) was used to detect the variation in physical appearance of annealed latex films. Monte Carlo simulations were performed to model the N and P fluorescence intensities (I_N and I_P) using photon diffusion theory. The number of N and P photons (N_N and N_P), emerging from the front surface of the latex film, are calculated when only N is excited where N_P photons are combined of photons from radiative (N_{PR}) and non-radiative (N_{PNR}) energy transfer processes. In simulations, annealing time, t, and the mean free path of a photon $\langle r \rangle$ are assumed to obey the Fickian diffusion model. A novel correction method was suggested, and employed to eliminate the P intensity due to the optical variation in latex film. P intensities from solely the energy transfer processes were monitored vs annealing time, and were used to measure the polymer chain diffusion coefficient (D), which was found to be 5.9×10^{-13} cm^2 s^{-1} at 180°C. © 1997 Elsevier Science Ltd.

(Keywords: fluorescence; interdiffusion; energy transfer; latex film; photon diffusion)

INTRODUCTION

The word interdiffusion in polymer science is used for the processes of mixing, intermingling and homogenization to the molecular level[1], which implies diffusion among distinguishable molecules. The process of interdiffusion deals with diffusion across boundaries, surfaces, interfaces and, sometimes, even gradients formed by the joining of bulk materials. Usually, when two pieces of an identical polymer are brought into intimate contact and heated above their glass transition temperature (T_g) the polymer chains become mobile, and interdiffusion of polymer molecules across the interface can occur.

Polymer interdiffusion measurements have usually emphasized the determination of diffusion coefficients in pure polymers, in blends, or in mixtures with solvents or other polymers. These measurements were usually performed using radioactive tracers[2], forward recoil spectroscopy (f.r.e.s.)[3], scanning electron microscopy (SEM), X-ray fluorescence[4], infra-red microdensitometry (i.r.m.)[5] and secondary ionization mass spectroscopy (s.i.m.s.)[6]. The major advantage of f.r.e.s. and s.i.m.s. is that the concentration profile produced through diffusion of the polymer across the interface can be determined directly.

Interdiffusion processes during latex film formation have been widely investigated over the past few years. These phenomena can be considered as special cases of crack healing or polymer welding processes. Latex films are formed from small polymer particles produced initially as a colloidal dispersion, usually in water. The term 'latex film' normally refers to a film formed from soft or low-T latex particles (T_g below room temperature) where the forces accompanying the evaporation of solvent are sufficient to deform the particles into a transparent, void-free film. Latex films can also be obtained by compression moulding of a dried latex powder composed of a polymer such as polystyrene (PS) or poly (methyl methacrylate) (PMMA) that has T_g above drying temperature. These latexes are generally called high-T particles. During drying process high-T latex particles remain essentially discrete and undeformed. The mechanical properties of such films can be evolved by annealing, which is called sintering of latex powder.

Recently, freeze fracture transmission electron microscopy (FFTEM) has been used to study the structure of dried latex films[7,8]. Small angle neutron scattering (SANS) has been used to study latex film formation at the molecular level. Extensive studies using SANS have been performed by Sperling and coworkers[9–11] on compression-moulded PS films. Using time-resolved fluorescence (t.r.f.) measurements in conjunction with dye-labelled particles, interdiffusion during latex film formation has been studied by Winnik and coworkers[12–15]. Direct non-radiative energy transfer (DET) was employed

* To whom correspondence should be addressed

to investigate the film formation processes in dye-labelled PMMA[12,15] and PBMA[13,14] systems. The DET method is particularly sensitive to the early stages, whereas the SANS technique becomes more sensitive to later stages of the interdiffusion processes. The steady state fluorescence (s.s.f.) technique combined with DET was recently used to examine healing and interdiffusion processes in dye-labelled PMMA latex films[16-18].

Because of photon diffusion, radiative and non-radiative energy transfer processes, special attention has to be paid during s.s.f. measurements to study the evolution of latex film formation. Film thickness and annealing time intervals are very critical for the quality of the film. In that sense photon diffusion, radiative and non-radiative processes compete and may play important roles during s.s.f. measurements. In this work, s.s.f. measurements were performed to study interdiffusion processes during film formation from PMMA particles, using DET.

The PMMA particles prepared by non-aqueous dispersion (NAD) polymerization. These particles were labelled with appropriate donor (naphthalene, N) and acceptor (pyrene, P) chromophores[19,20]. The 1–3 μm diameter particles were used having two components; the major part, PMMA, comprises 96 mol% of the material, and the minor component, polyisobutylene (PIB) (4 mol%), forms an interpenetrating network through the particle interior[21,22], very soluble in certain hydrocarbon media. A thin layer of PIB covers the particle surface and provides colloidal stability by steric stabilization. (These particles were prepared in Professor M. A. Winnik's laboratory in Toronto.)

In this paper two sets of isothermal experiments were performed by annealing PMMA latex film samples at 180°C, in elevated time intervals. In the first set, after annealing, only P was excited at 345 nm and emission intensity (I_{op}) was observed vs annealing time. This set of experiments were performed to detect the evolution of the quality (transparency) of the film samples. During the second set of experiments, after annealing the film samples, N and P intensities (I_N and I_P) were monitored against annealing time, when the films were excited at 286 nm. In this set of experiments we aimed to observe the chain interdiffusion across the particle–particle junction. Monte Carlo simulations were carried out to model the I_{op}, I_N and I_P intensities emitted from latex film, using photon diffusion theory. A novel correction method was suggested and employed to separate the P intensity (I_P) due to nonradiative and radiative energy transfer, from the total P intensity, I_P, which produced the characteristics of chain interdiffusion. In these simulations, annealing time, t, and the mean free path of a photon, $\langle r \rangle$ are assumed to obey the Fickian diffusion model as $\langle r \rangle \propto t^{1/2}$.

EXPERIMENTAL

NP-labelled PMMA-PIB polymer particles were prepared separately in a two-step process in which MMA was polymerized in the first step to low conversion in cyclohexane, in the presence of PIB containing 2% isoprene units to promote grafting. The graft copolymer so produced served as a dispersant in the second stage of polymerization, in which MMA was polymerized in a cyclohexane solution of the copolymer. Details have been published[19]. A stable spherical dispersion of polymer particles was produced, ranging in radius from 1 to 3 μm. A combination of ^{1}H nuclear magnetic resonance (n.m.r.) and ultraviolet (u.v.) analysis indicated that these particles contain 6 mol% PIB and 0.37 mmol N and 0.037 mmol P groups per gram of polymer. We refer to these particles as N and P respectively.

Latex film preparation was carried out as follows; the same weights on N and P particles were dispersed in heptane in a test tube; after complete mixing, a large drop of the dispersion was placed on a round silica window plate with a diameter of 2 cm. Heptane was allowed to evaporate and the silica window was placed in the solid surface accessory of a Perkin Elmer Model LS-50 fluorescence spectrometer. All measurements were carried out in the front face position at room temperature. Slit widths were kept at 2.5 mm. The N–P film sample was excited at 286 nm in order to maximize napthalene absorbance while minimizing pyrene absorbance. Film samples were illuminated only during the actual fluorescence measurements and, at all other times, were shielded from the light source. The film of latex particles was annealed above the T_g of PMMA for various periods of time at 180°C. The temperature was maintained within ±2° during the annealing. The variation in optical density of N–P film was controlled by only exciting pyrene at 345 nm for each measurement. SEM measurements were performed with a JEOL JSM T330 system. A Hummer VII sputtering system was used for gold coating, and latex particles were examined at 15 kV.

THEORETICAL CONSIDERATIONS

Photon diffusion model and DET

The journey of an exciting or emitted photon to or from a dye molecule in a film formed from annealed latex particles can be modelled by photon diffusion theory[23]. The collision probability, P, of a travelling photon with any scattering centre in a film is given by

$$P = 1 - \exp(-r\langle r \rangle) \tag{1}$$

where r is the distance of a photon between each consecutive collision and $\langle r \rangle$ is defined as the mean free path of a photon. Here the film is taken as a plane sheet with a thickness of d, and the direction of incident photons is taken perpendicular to the film surface (for example in direction z). In Monte Carlo simulations, d after each collision is compared with the z component of the total distance

$$s_z = \sum_i^n r_{iz} \tag{2}$$

where i labels the successive collisions during the journey of a photon. Photons emerging from the back and front surface of the film without interacting with a pyrene molecule have to satisfy the conditions given below

$$s_z > d \quad \text{and} \quad s_z < 0 \tag{3}$$

respectively. The total number of photons emerging from the front surface is then represented by N_{sc}, which is assumed to be proportional to the intensity, I_{sc} of the light scattered from latex film during s.s.f. measurements.

When the interaction of a photon with a dye molecule

is considered, mainly two types of Monte Carlo simulations can be carried out. At first, the number of photons (N_{op}) emitted from the front surface of the latex film is calculated when only P molecules are excited, which models the direct emission intensity from pyrene (I_{op}). In the second part, the number of photons-emitted from the latex film is calculated when only Ns are excited. In this part of the simulation non-radiative and radiative energy transfer processes are considered, and N and P emissions (I_N and I_P) were modelled by counting N and P photons (N_N and N_P) emitted from the front surface of the film.

In order to drive the relation for the fluorescence intensity, I_{op} emitted from the latex film, we defined the probability of a photon encountering a pyrene molecule to be,

$$q = 1 - \exp(s/l) \tag{4}$$

Here s represents the total distance (optical path) and l is the mean distance the photon travels in the film, before it finds a pyrene molecule. If s is large, the probability of the photon encountering a P is high, or vice versa. After collision with a P molecule the photon travels again according to equation (1). Then, d is compared with the z component of the total distance, s_z as in equation (3), to find if the photon is emitted from the film surfaces. The number of photons emitted from the front surface of the film is given by N_{op}, which is assumed to be proportional to I_{op}, the fluorescence intensity. In Monte Carlo simulations l and d were taken to be fixed parameters with values of 150 and 50 respectively. Here we have to note that l is considered to be proportional to the P concentration in latex film, which is assumed to be constant during the film formation processes. The mean free path, $\langle r \rangle$, was varied between 1 and 100 for a given d, and for each $\langle r \rangle$ the number of incident photons was taken to be 3×10^4 during the simulations. The number of collisions, n, is varied so that the conditions in equation (2) are satisfied.

In the second part of the Monte Carlo simulations, the probability of a photon encountering a naphthalene molecule can be defined as

$$P_N = 1 - e^{s_N/l_N} \tag{5}$$

Here, s_N is the total distance, and l_N the mean distance, the photon travels in the film, before it finds a N molecule. After collision with a N, the photon travels again by satisfying equation (1), and is emitted from the film surfaces according to equation (3). The number of N photons emitted from the front surface of the film is given by N_N, and is assumed to be proportional to I_N, the N fluorescence intensity. There is always a certain probability of a N photon encountering a P molecule, which is defined by

$$P_P = 1 - e^{-s_P/l_P} \tag{6}$$

This process is called 'radiative energy transfer', where s_p represents the total distance and l_p is the mean distance, the N photon travels in the film, before it finds a P molecule. In equations (5) and (6) l_N and l_P are considered to be inversely proportional to the naphthalene and pyrene concentrations in latex film. Here, again after collision, the photon travels by satisfying equation (1) and is emitted from the film surface according to equation (3). After the radiative energy transfer has taken place, the number of pyrene photons emitted from the front surface of the film is given by N_{PR}. During simulations l_N and l_P are taken to be fixed parameters with values of 100 and 1000 respectively.

When the distance between N and P molecules is short enough they can interact, and an excited N molecule can transfer its energy to a nearby P molecule, before emitting a photon. This process is called DET. This mechanism is known as a dipolar Förster interaction in photophysics terminology. During film formation from latex particles, P- and N-labelled chains interdiffuse and can form a Förster domain where an excited N molecule can transfer its energy to a P molecule with 90% probability (experimentally determined from the completely mixed, chloroform cast films). Then the excited P molecule releases a photon, which travels by satisfying equation (1) and is emitted from the film surface according to equation (3). After the DET, the number of P photons emitted from the front surface of the film is represented by N_{PNR}. A cartoon representation of interdiffusing polymer particles is given in *Figure 1*, where at $t = 0$, before interdiffusion starts, only N emission takes place. However as the interdiffusion proceeds, even only N molecules are excited, at $t > 0$ P photons are created in the mixed 'Förster region' (shaded area) due to the non-radiative energy transfer. The total number of P photons emitted from the front surface of the film is then given by $N_P = N_{PR} + N_{PNR}$.

Modelling interdiffusion by fluorescence

The interdiffusion process in polymers can be explained by several theories[24-26] that are based on the reptation model of de Gennes[27]. In the bulk state polymer chains have a Gaussian distribution of segments. When chains are confined to the space adjacent to the interface, they have distorted conformations. Interdiffusion across the interface leads to conformational randomization and recovery of a Gaussian distribution

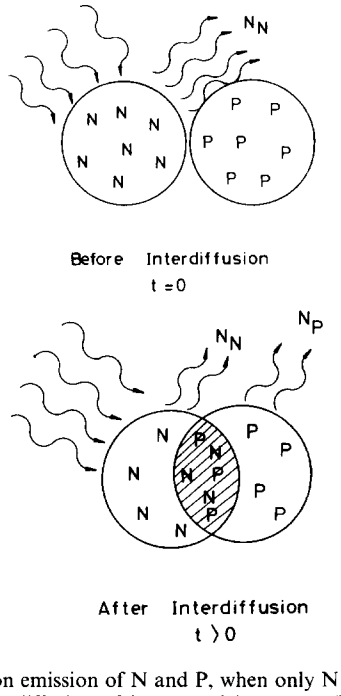

Figure 1 Photon emission of N and P, when only N is excited: (a) at $t = 0$ before interdiffusing of latex particles starts; (b) at $t > 0$ after interdiffusion of latex particles starts. N_N and N_P are the numbers of N and P photons emitted from the front surface of the latex film

of segments[28,32]. Entanglements prevent macromolecules larger than a certain (critical) length from undergoing large amplitude sideways diffusion. These macromolecules are pictured as being confined to a tube, and their diffusion occurs by coherent back and forth motion along the centre line of the tube with a curvilinear diffusion coefficient, keeping the arc length of the chain constant. This worm-like motion is referred to as 'reptation'. The reptation time, T_r, is the time necessary for a polymer to diffuse a sufficient distance so that all memory of the initial tube is lost. The diffusion rate of this reptation across a polymer–polymer interface should be sensitive to the location of the chain ends. Since there is more free volume at the interface than in the bulk, an enrichment of chain ends at the interface is expected.

Tirrell *et al.*[29] studied interdiffusion in terms of the s.s.f. of an acceptor emission intensity due to DET from a donor. In our case the DET process can be represented by:

$$N^* + P \rightarrow N + P^* \qquad (7)$$

Here N^* and P^* are the excited N and P molecules respectively. When the donor is excited exclusively, and can transfer its energy to nearby acceptor groups, the fluorescence intensity of the acceptor, $I(t)$, increases with time:

$$I(t) - I(0) = I_0 \alpha \int_{-\infty}^{+\infty} C(x,t)[C_0 - C(x,t)]\,dx \qquad (8)$$

where $I(0)$ is $I(t)$ at time zero, and the x-axis is taken as normal to the polymer–polymer interface. Here I_0 represents the incident light intensity, α is a constant, $C(x,t)$ is the concentration profile of an acceptor at time t, and C_0 is its interface concentration. At times longer than T_r, concentration profiles can be obtained from Fick's law of diffusion[33]

$$\frac{\partial C(r,t)}{\partial t} = D\nabla^2 C(r,t) \qquad (9)$$

Then equation (8) can be rewritten as[29]:

$$I(t) - I(0) = 0.165\alpha C_0^2 (Dt)^{1/2} \qquad (10)$$

where D is the centre of mass diffusion coefficient of the polymer chain.

RESULTS AND DISCUSSION

Film quality and photon diffusion

Typical emission (I_{op}) and scattered (I_{sc}) spectra of a latex film annealed at 180°C in elevated time intervals and excited at 345 nm, are shown in *Figure 2*. Upon annealing, P intensity (I_{op}) increased for a 15 min interval, then decreased by increasing time intervals. However, I_{sc} decreased continuously from the beginning by increasing annealing time. The behaviours of (I_{op}) and (I_{sc}) vs annealing time are plotted in *Figures 3a* and *3b* respectively. The maximum in I_{op} can be explained by the two-stage healing processes[18,34], at the particle–particle junction where the polymer chains try to relax across the junction surface. Time 15 min can be referred to as the healing time (τ_H) at 180°C, during which the chains move halfway across the interface surface and occupy all the interparticle voids. At this temperature and time, the original particle boundaries disappear, and consequently

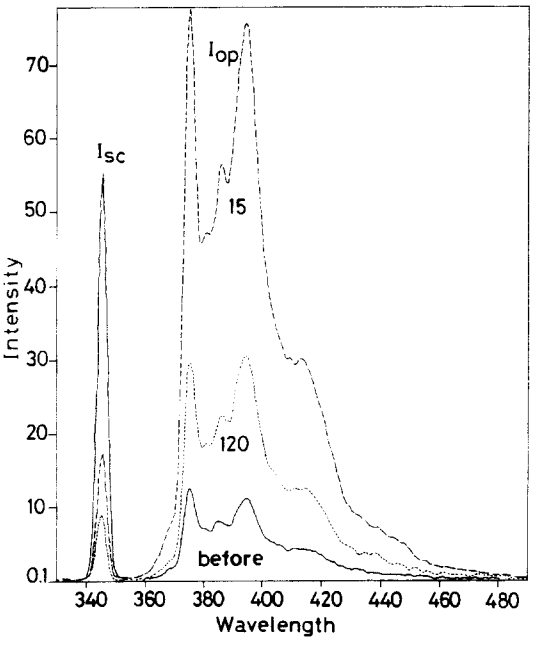

Figure 2 Emission (I_{op}) and, scattered (I_{sc}) spectra of a latex film before annealing, and annealed at 180°C in 15 and total 120 min time intervals. Film is formed from N and P particles and excited at 345 nm

latex film starts to become semi-transparent to the exciting light for P molecules. As a result, the emission intensity I_{op} reaches a maximum. The variation in I_{op} depends on the optical path, s, of a photon in the film. This optical path is directly proportional to the probability of the photon encountering a P molecule. Before annealing, the photon is scattered from the particle surfaces. The mean free path, $\langle r \rangle$, is of the order of the size of the inter-particle voids, and after a few steps, the photon reemerges from the front surface of the film. Thus, the optical path, s, is very short. Once the first stage of the healing process is completed, scattering is predominantly from the interparticle interfaces and the mean free path becomes of the order of the particle size. Clearly, in this regime, with the same number of re-scatterings, a photon will spend a much longer time in the film, and consequently, I_{op} becomes a maximum. After the completion of the second stage of the healing process, however, these interfaces are also removed. The film starts to become essentially transparent to the photon,

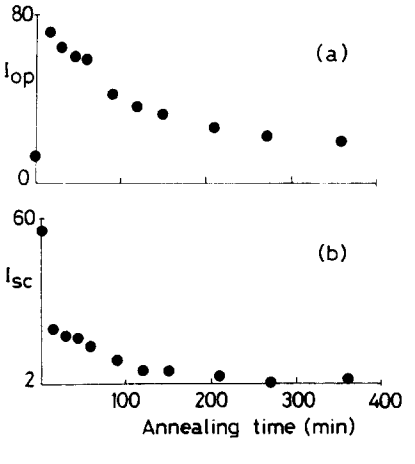

Figure 3 Variation of: (a) (I_{op}); (b) (I_{sc}), intensities vs annealing time. Film is excited at 345 nm

the mean free path diverges, and s then becomes of the order of the film thickness, d. We have demonstrated, by mean of Monte Carlo simulations to be discussed below, that merely the film thickness represents a much shorter value of the optical path than that obtained by multiple scattering from interfaces after the first stage of the healing process. Hence, the decrease in I_{op} after complete annealing has occurred.

These speculations can be quantitatively modelled and the behaviour of (I_{op}) and (I_{sc}) can be interpreted by the results of Monte Carlo simulations. N_{op} and N_{sc} are plotted vs the square of the mean free path ($\langle r\rangle^2$) of a photon in *Figures 4a* and *4b* respectively. Here it is assumed that the relation $\langle r\rangle = \sqrt{DT}$ is obeyed, where t is the annealing time and D is given in equation (9). As a result, when the annealing time increases, the square of the mean free path increases. In *Figure 4a*, N_{op} first increases suddenly then decreases by increasing $\langle r\rangle^2$. These indicate that for very short $\langle r\rangle^2$ values, s is short, but as $\langle r\rangle^2$ values increase the optical path, s, of a photon becomes longer and the probability of encountering a P in the film is higher. As a result, N_{op} reaches a maximum. However, for longer $\langle r\rangle^2$ values, s becomes shorter again and photons can easily escape from the back surface of the film and both N_{op} and N_{sc} decrease continuously by increasing $\langle r\rangle^2$ values.

In order to support these findings SEMs of latex films were taken, before and after annealing above T_g for 15 and 6 × 15 min time intervals, and presented in *Figure 5*. *Figure 5a* shows the SEM result of a powder film before annealing. *Figure 5b* presents a film annealed at 180°C for 15 min, where disappearance of particle boundaries can be seen. An almost transparent film obtained by annealing at 180°C for 6 × 15 min intervals is shown in *Figure 5c*. The film in *Figure 5a* shows the lowest I_{op} value, however the film of *Figure 5b* gives the highest I_{op} value. The corresponding I_{sc} intensities of film samples in *Figure 5* show a decrease by increasing annealing time intervals. SEM results are found to be consistent with the photon diffusion model. Cartoon representations of film formation from high-T latex particles and its relation with the mean free and optical paths ($\langle r\rangle$ and s) are presented in *Figure 6*. The early stage of film formation is shown in *Figure 6a*, where heptane evaporates and close packed particles form a powder film which includes many voids. This film yields low I_{op} and high I_{sc} values due to very short $\langle r\rangle^2$ and short s values. *Figure 6b* shows a film where, due to annealing, particle boundaries start to heal and disappear, which gives rise to short $\langle r\rangle^2$ and the longest s values. In such a film one can observe high I_{op} and low I_{sc} intensities. Finally *Figure 6c* shows an almost transparent film with the longest $\langle r\rangle^2$ but smaller s values. This film naturally presents both low I_{op} and I_{sc} intensities.

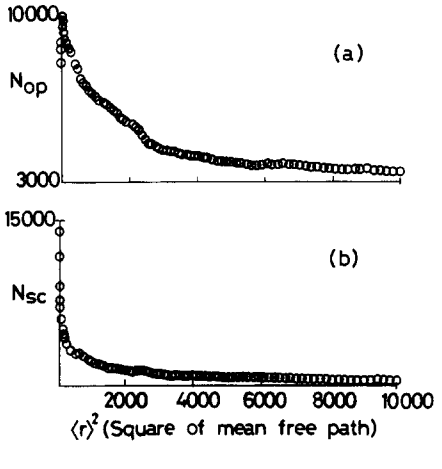

Figure 4 Variation of: (a) (N_{op}); (b) (N_{sc}), vs $\langle r\rangle^2$, square of mean free path of a photon. Results are obtained from Monte Carlo simulations

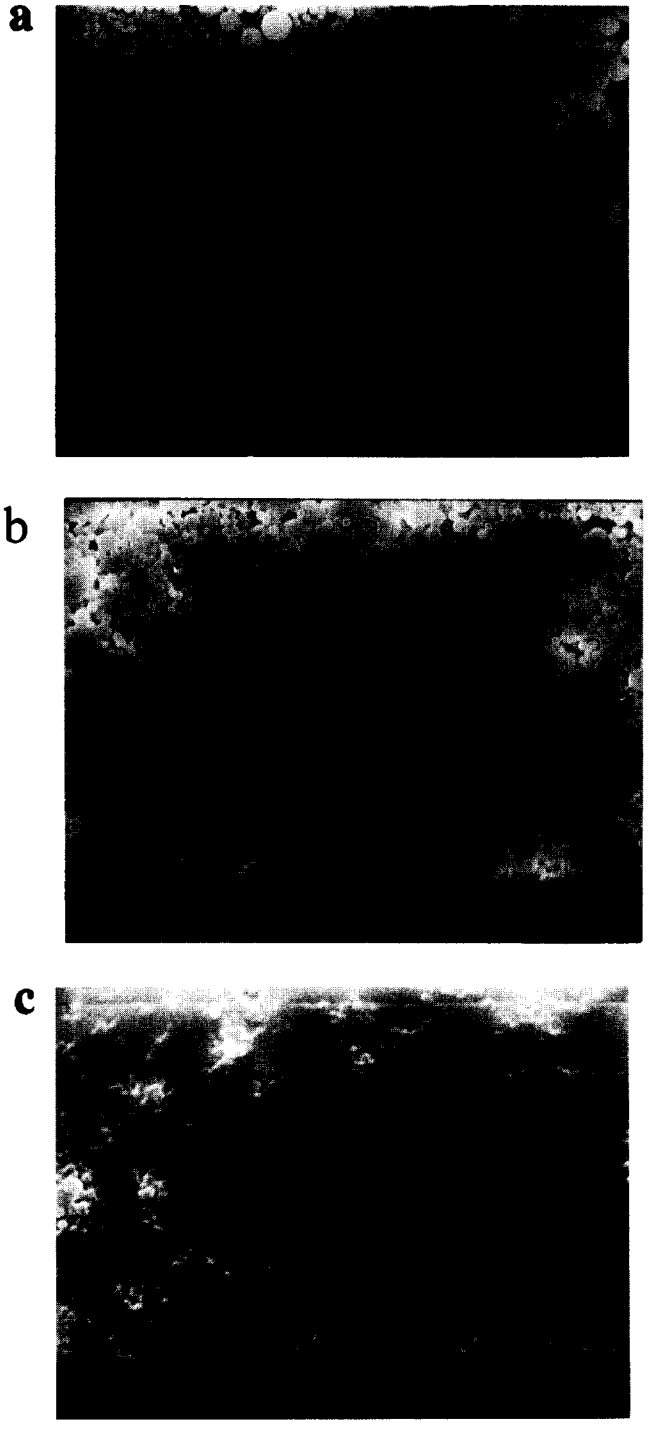

Figure 5 SEM results of latex films: (a) before annealing; (b) annealed at 180°C for 15 min; (c) annealed at 180°C for 6 × 15 min time intervals

Monte Carlo simulations for energy transfer processes

When the interdiffusion process of polymer chains proceeds, particle boundaries disappear and DET between N and P molecules takes place. This picture

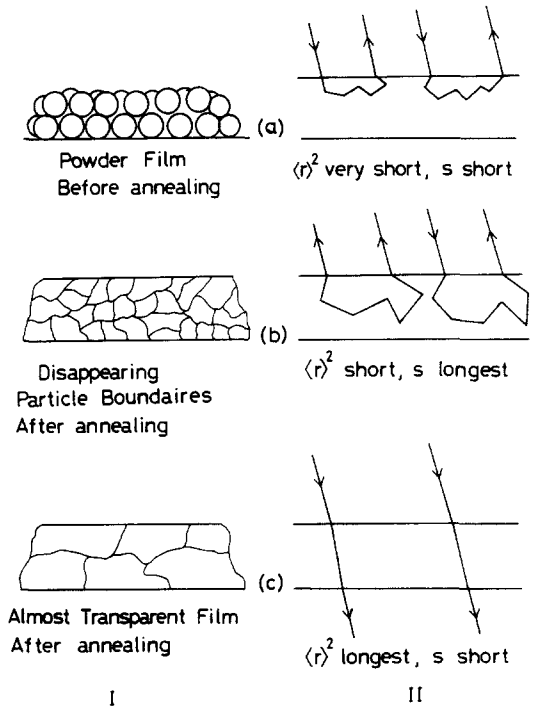

Figure 6 Cartoon representation of latex film formation from high-T latex particles: (a) before annealing, powder film; (b) annealed film, beginning of disappearance of particle boundaries; (c) highly annealed, almost transparent film

can be quantitatively modelled by the results of Monte Carlo simulations. The total number of P and N photons (N_P and N_N) emitted from the front surface of the film are plotted vs $\langle r\rangle^2$ of a photon in *Figures 7a* and *b* respectively, where N_P decreases continuously. However, N_N increases at the beginning and then decreases by increasing $\langle r\rangle^2$. As the annealing time, t, increases, $\langle r\rangle^2$ also increases due to the disappearance of interparticle voids and interfaces. Then one should expect an increase in P and a decrease in N intensities, due to energy transfer from N to P molecules. Since N_P contains photons from both radiative and non-radiative processes, the above contradiction can be resolved using Monte Carlo simulations. *Figures 8a* and *8b* show the plot of N_{PR} and N_{PNR} *versus* $\langle r\rangle^2$, where one can observe a continuous increase in N_{PNR} photons due to a non-radiative energy transfer process from N to P molecules.

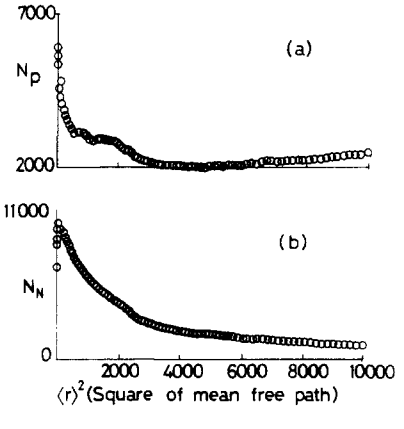

Figure 7 Variation of total number of: (a) P (N_P); (b) N (N_N), photons vs $\langle r\rangle^2$, square of mean free path of a photon. Results are obtained from Monte Carlo simulations

The number of photons due to the radiative energy transfer (N_{PR}) process presents very high values at the beginning of film formation, then decreases immediately due to the increase in $\langle r\rangle$ values. Now *Figures 7b* and *8b* look consistent, by showing a decrease in N photons and an increase in P photons respectively, but still this correspondence is not one-to-one. In other words, this picture still does not fit Tirrel's model of equations (7) and (8). Here, emission from N due to variation in film quality (N_{OP}) dominates the total N_N emission. This contribution can be rationalized by comparing *Figure 7b* and *Figure 4a*, where the quality of the film (or $\langle r\rangle$) affects the number of emitted photons in both cases. In order to eliminate the photons (N_{op}) created due to the variation in the quality of the film, and to separate the contributions solely from the radiative and non-radiative energy transfer processes, we normalize the total number of photons emitted from the front surface of the film as follows

$$N'_P + N'_N = 1000 \qquad (11)$$

where N'_P and N'_N are the normalized total number of P and N photons emitted from the front surface of the film respectively. N'_P and N'_N are plotted vs $\langle r\rangle^2$ of a photon in *Figures 9a* and *9b* respectively, in which one to one

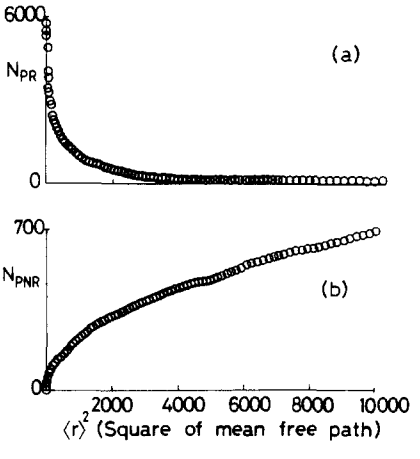

Figure 8 Variation of number of: (a) P photons (N_{PR}) due to radiative transfer; (b) P photons (N_{PNR}) due to non-radiative transfer from N to P molecules, emitted from the front surface of the film

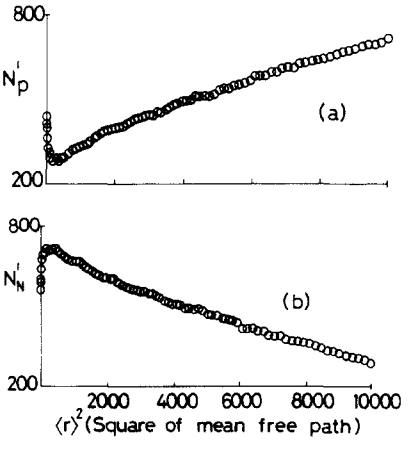

Figure 9 Variation of normalized total number of (a) P (N'_P); (b) N (N'_N), photons *versus* $\langle r\rangle^2$, square of mean free path of a photon. Normalization is done according to equation (11)

correspondence between P and N emissions now can be seen. When *Figure 8b* is compared with *Figure 9a*, it is seen that N'_P is created by a non-radiative energy transfer process (N_{PNR}), except at very early N_{PR} contribution. The normalized photon emissions from naphthalene N'_N now decrease due to non-radiative energy transfer from N to P as the mean free path $\langle r \rangle$ of a photon increases, except at the early stage of radiative energy transfer contribution.

Chain interdiffusion

The emission spectra of a mixture of N- and P-labelled latex films before and after annealing at 180°C for 15 and total 120 min time intervals are shown in *Figure 10*, where the film is excited at 286 nm. The solid line indicates the spectrum before annealing. The scattered intensity, I_{SC}, is also presented on the left hand side of *Figure 10*. I_P and I_N both increase suddenly by annealing the film sample for 15 min, then decrease continuously by increasing annealing time intervals. However, the I_{SC} intensity decreases continuously from the beginning by increasing annealing time. The variation in I_N and I_P intensities vs annealing time are shown in *Figure 11*. From the point of view of DET, the decrease in I_N is expected, but the decrease in I_P is quite surprising. One would naturally expect an increase in I_P due to DET processes as I_N decreases. In the previous section, Monte Carlo simulations have predicted that this anomalous behaviour in I_P is produced due to the variation in the quality of the film, which can be resolved by using equation (11). The emission due to the variation in optical quality of the film can be eliminated by normalizing the total P and N intensities to 1000. The variation in normalized P and N intensities (I'_P and I'_N) vs annealing time are presented in *Figures 12a* and *12b* respectively. As expected from Monte Carlo simulations, as I'_P now increases, I'_N decreases by increasing annealing time. This behaviour in I'_P and I'_N intensities show one-to-one correspondence, which indicates that the energy

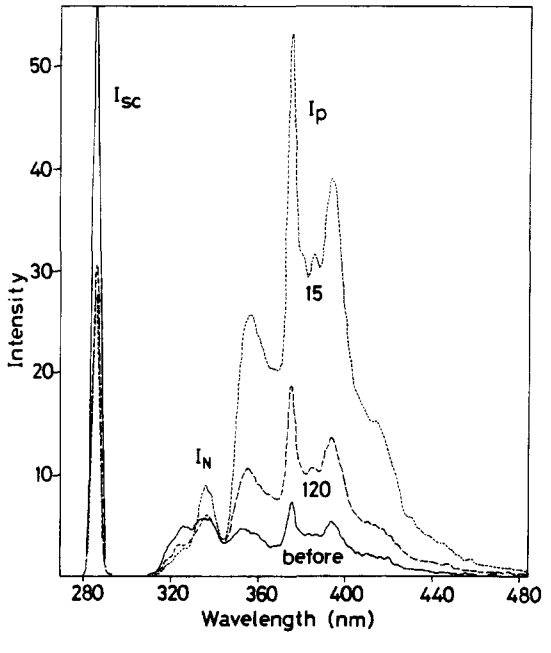

Figure 10 Emission (I_N and I_P) and scattered (I_{sc}) spectra of a latex film before and after annealing at 15 and total 120 min time intervals at 180°C. Film is formed from N and P particles and excited at 286 nm

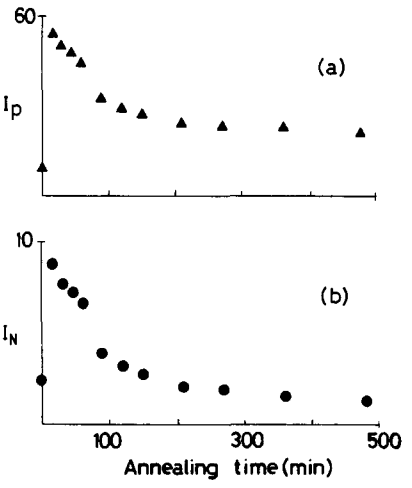

Figure 11 Variation of: (a) P(I_P) and (b) N (I_N), intensities vs annealing time. Film is excited at 286 nm

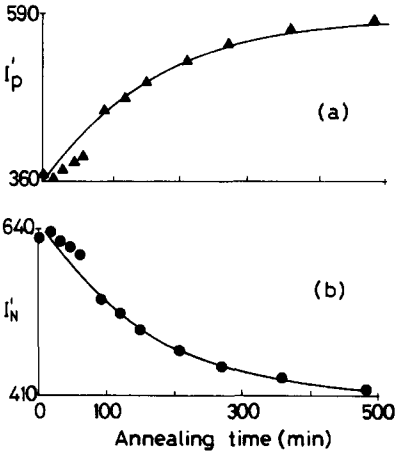

Figure 12 Variation of normalized (a) (I_P); (b) N (I'_N), intensities vs annealing time. Normalization is performed using the $(I'_P + I'_N) = 1000$ relation

transfer processes between N and P are purely radiative and non-radiative. In order to quantify the above results, equation (10) can be used for I'_P intensity as follows

$$\frac{I'_P(t) - I'_P(0)}{I'_P(\infty) - I'_P(0)} = \frac{(Dt)^{1/2}}{R} \qquad (12)$$

Here, R is the radius of the particle and $I'_P(\infty)$ is the P intensity at $t = \infty$. Equation (12) is fitted to the data in *Figure 12a*, and the chain diffusion coefficient, D, is produced from the slope of this fit in *Figure 13a*. The linear relation in *Figure 13* supports Tirrel's model, given above, where Fickian type diffusion is considered for times longer then the reptation time T_r of the polymer chain. The diffusion coefficient that was observed in this work is found to be $D = 5.9 \times 10^{-13}\ cm^2\ s^{-1}$, which is an order of magnitude faster than was observed in the similar system at 170°C using transient fluorescence technique[12].

The linear curve in *Figure 13* does not go through the origin, which means that there is a delay in chain interdiffusion which may correspond to a healing time (τ_H)[18]. It is mentioned above that, during the first 15 min, chains move halfway across the interface surface and

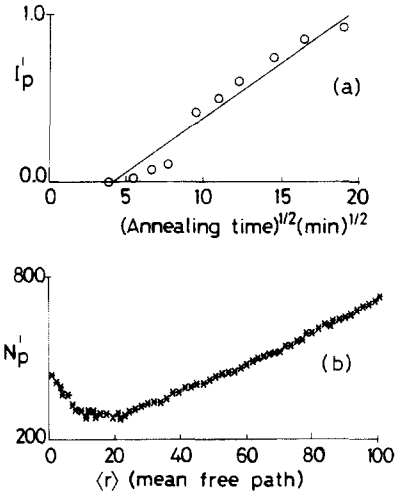

Figure 13 (a) Plot of the data in *Figure 12a* vs square root of annealing time. Slope of the linear plot produced diffusion coefficient as $D = 5.9 \times 10^{-13}$ cm^2 s^{-1}. (b) Plot of the data in *Figure 9a* vs $\langle r \rangle$, mean free path of a photon

particle boundaries start to disappear. This picture can be visualized by the result of the Monte Carlo simulation. When the normalized total number of photons, N'_P, is plotted against the mean free path of a photon, $\langle r \rangle$, which now corresponds to (time)$^{1/2}$, it is seen that a certain delay is required for non-radiative energy transfer to start. *Figure 13b* presents the plot of N'_P vs $\langle r \rangle$, where at the beginning, for very short $\langle r \rangle$ values, the number of P photons due to radiative energy transfer (N_{PR}) dominates to N'_P, then N'_P decreases by increasing $\langle r \rangle$. As $\langle r \rangle$ values continue to increase, which is equivalent to saying that interdiffusion increases in time, the number of P photons due to DET (N_{PNR}) increase, and as a result N'_P increases.

In conclusion, the simple s.s.f. method has been used to measure backbone diffusion coefficient, D, during film formation from high-T latex particles, where the experiments are easy to perform and spectrometer is inexpensive to obtain. Monte Carlo simulations have been performed to introduce a novel correction tech nique to the energy transfer measurements for the s.s.f. method which is very appropriate for measuring D values.

ACKNOWLEDGEMENT

We thank The Turkish Academy of Sciences (TÜBA) for their financial support, and Professor M. A. Winnik for providing us with the latex material.

REFERENCES

1. Kausch, H. H. and Tirrell, M., *Annu. Rev. Mater. Sci.*, 1989, **19**, 341.
2. Bueche, F., *Chem. Phys.*, 1970, **48**, 1410.
3. Tead, S. F. and Kramer, E. J., *Macromolecules*, 1988, **21**, 1513.
4. Jones, R. A. L., Klein, J. and Donald, A. M., *Nature*, 1986, **321**, 161.
5. Klein, J., *Science*, 1990, **250**, 640.
6. Whitlow, S. J. and Wool, R. P., *Macromolecules*, 1991, **24**, 5926.
7. Wang, Y., Kats, A., Juhue, D., Winnik, M. A., Shivers, R. R. and Dinsdale, C. J., *Langmuir*, 1992, **8**, 1435.
8. Roulstone, B. J., Wilkinson, M. C., Hearn, J. and Wilson, A. J., *Polym. Int.*, 1991, **24**, 87.
9. Linne, M. A., Klein, A., Miller, G. A., Sperling, L. H. and Wignall, G. D., *Macromol. Sci., Phys., B2*, 1988, **2–3**, 217.
10. Yoo, J. N., Sperling, L. H., Glinka, C. J. and Klein, A., *Macromolecules*, 1990, **23**, 3962.
11. Kim, K. D., Sperling, L. H. and Klein, A., *Macromolecules*, 1993, **26**, 4624.
12. Pekcan, Ö., Winnik, M. A. and Croucher, M. D., *Macromolecules*, 1990, **23**, 2673.
13. Wang, Y., Zhao, C. and Winnik, M. A., *J. Chem. Phys.*, 1991, **95**, 2143.
14. Wang, Y. and Winnik, M. A., *J. Phys. Chem.*, 1993, **97**, 2507.
15. Wang, Y. and Winnik, M. A., *Macromolecules*, 1993, **26**, 3147.
16. Pekcan, Ö., Canpolat, M. and Göçmen, A., *Eur. Polym. J.*, 1993, **29**, 115.
17. Pekcan, Ö., Canpolat, M. and Göçmen, A., *Polymer*, 1993, **34**, 3319.
18. Canpolat, M. and Pekcan, Ö., *Polymer*, 1995, **36**, 2025.
19. Winnik, M. A., Hua, M. H., Hongham, B., Williamson, B. and Croucher, M. D., *Macromolecules*, 1984, **17**, 262.
20. Pekcan, Ö., Winnik, M. A. and Croucher, M. D., *J. Colloid Interface Sci.* 1983, **95**, 420.
21. Pekcan, Ö., Egan, L. S., Winnik, M. A. and Croucher, M. D., *Phys. Rev. Letts*, 1988, **61**, 641.
22. Pekcan, Ö., Egan, L. S., Winnik, M. T. and Croucher, M. D. *Macromolecules*, 1990, **23**, 2210.
23. Meeten, G. H., *Optical Properties of Polymers*. Elsevier Science, New York, 1989.
24. de Gennes, P. G., *Macromolecules*, 1976, **11**, 587.
25. Doi, M. and Edward, S. F., *J. Chem. Soc., Faraday Trans. 2*, 1978, **74**, 1802.
26. Klein, J., *Macromolecules*, 1978, **11**, 852.
27. de Gennes, P. G., *Chem. Phys.*, 1971, **75**, 5194.
28. Prager, S. and Tirrell, M., *Chem. Phys.*, 1981, **75**, 5194.
29. Tirrell, M., Adolf, D. and Prager, S., *Springer Lecture Notes, Appl. Math.*, 1984, **37**, 1063.
30. Wool, R. P. and O'Connor, K. M., *J. Appl. Phys.*, 1981, **52**, 5953.
31. Wool, R. P. Yuan, B. L. and McGarel, O. J., *Polym. Eng. Sci.*, 1989, **29**, 1340.
32. Kim, Y. H. and Wool, R. P., *Macromolecules*, 1983, **16**, 1115.
33. Crank, J., *The Mathematics of Diffusion*. Clarendon Press, Oxford, 1975.
34. Pekcan, Ö., *Trends Polym. Sci.*, 1994, **2**, 236.